Imprint of double-detonation mechanism in early light curves for Type Ia supernovae

Petr Baklanov (ITEP)

with Noebauer U., Blinnikov S., Sorokina E.,
Kromer M., Taubenberger S., Hillebrandt W. (MPA)

APEC Seminar
Kavli IPMU

Jan 31, 2019

Outline

- Motivations
- Review of the models
  - Carbon deflagration W7
  - Delayed detonation (N100)
  - Violent merger (merger)
  - Sub-Chandrasekhar mass detonation (SubChDet)
  - Double detonation scenario (SubChDoubleDet)
- Modelling early light curves with code STELLA
- Early light curves and their features
- Imprints of double-detonation mechanism in early LCs
- Conclusions

Thermonuclear (Type Ia) supernovae:

- They do not have hydrogen lines and have strong Si lines in the spectrum.
- They are found in all types of galaxies, including elliptical.
- They are the most common type. Most SNe, 60%, are of type Ia
- They can be used as distance indicators.
- They are likely result of thermonuclear explosion of CO WDs. However, details of the progenitor stars and explosion mechanisms are still uncertain and various models are discussed.

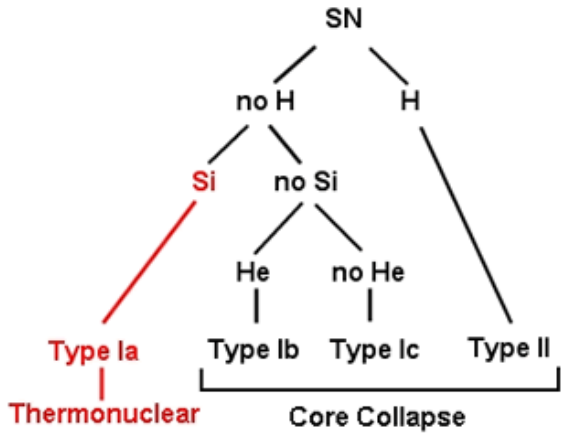

via http://astronomy.swin.edu.au

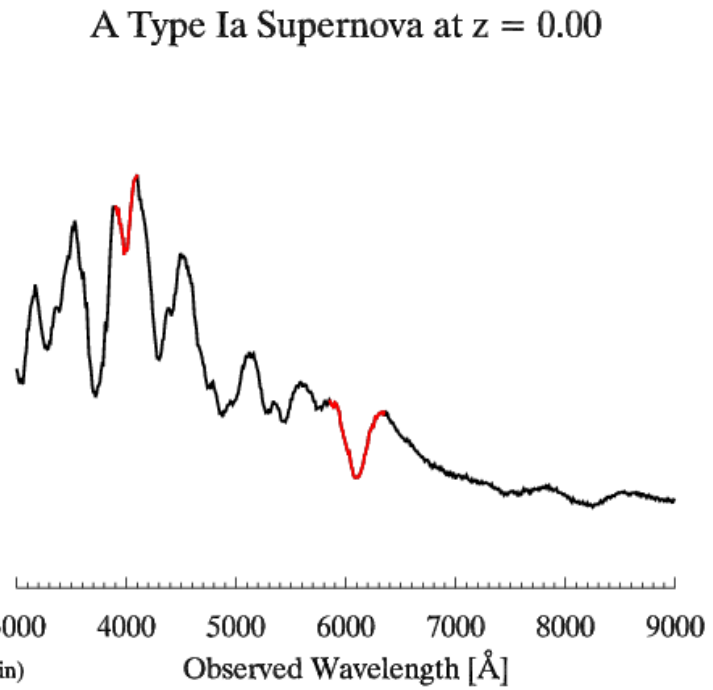

Thermonuclear (Type Ia) supernovae:

- They do not have hydrogen lines and have strong Si lines in the spectrum.
- They are found in all types of galaxies, including elliptical.
- They are the most common type. Most SNe, 60%, are of type Ia
- They can be used as distance indicators.
- They are likely result of thermonuclear explosion of CO WDs. However, details of the progenitor stars and explosion mechanisms are still uncertain and various models are discussed.

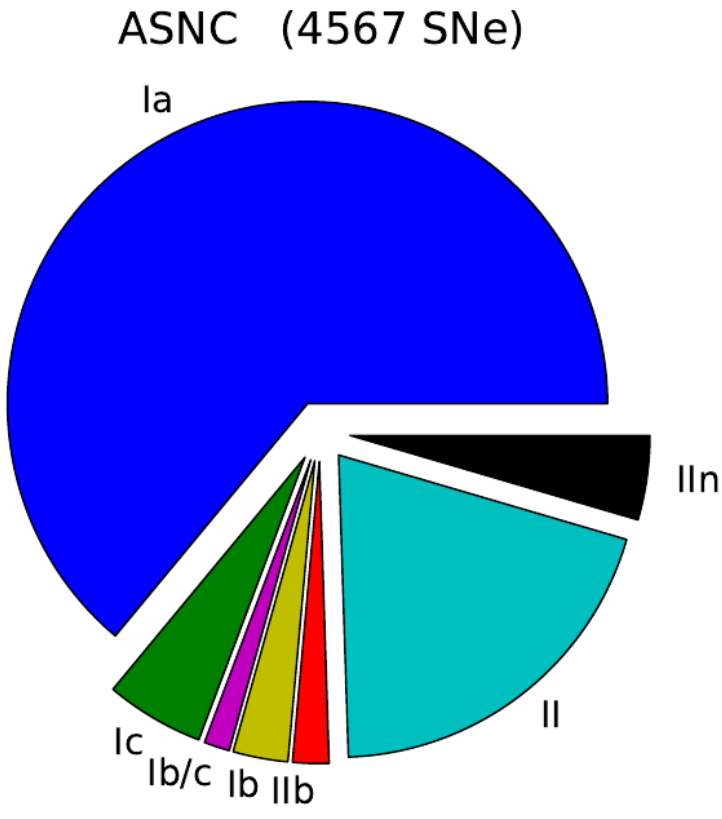

via arXiv:1403.7233

Thermonuclear (Type Ia) supernovae:

- They do not have hydrogen lines and have strong Si lines in the spectrum.
- They are found in all types of galaxies, including elliptical.
- They are the most common type. Most SNe, 60%, are of type Ia
- They can be used as distance indicators.
- They are likely result of thermonuclear explosion of CO WDs. However, details of the progenitor stars and explosion mechanisms are still uncertain and various models are discussed.

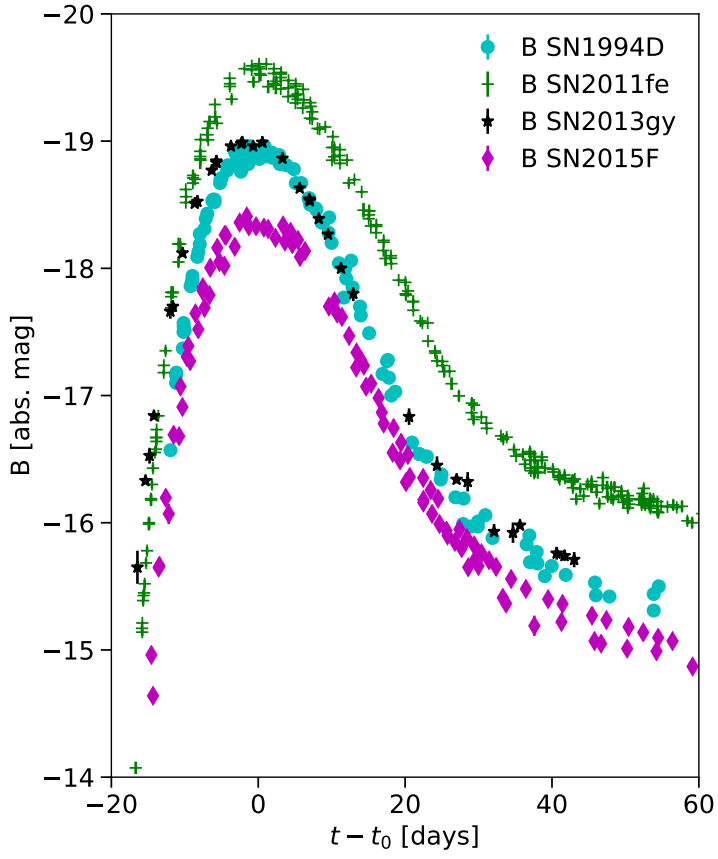

Thermonuclear (Type Ia) supernovae:

- They do not have hydrogen lines and have strong Si lines in the spectrum.
- They are found in all types of galaxies, including elliptical.
- They are the most common type. Most SNe, 60%, are of type Ia
- They can be used as distance indicators.
- They are likely result of thermonuclear explosion of CO WDs. However, details of the progenitor stars and explosion mechanisms are still uncertain and various models are discussed.

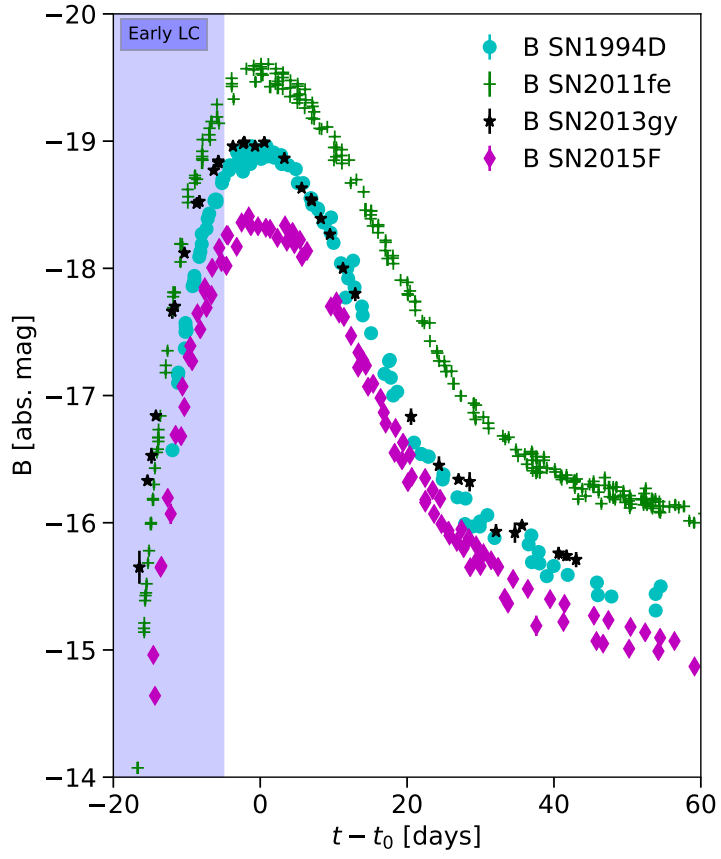

A set of detailed explosion models of SNe Ia

Single degenerates (SD)

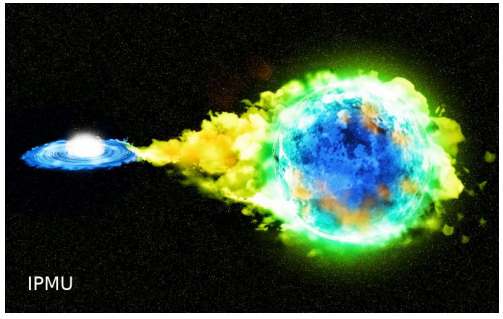

- W7 – carbon deflagration model by Nomoto (1984), a standard theoretical reference model for SN Ia
- N100 – delayed detonation model. The thermonuclear flame first propagates as a subsonic deflagration which later transitions into a detonation.

Double degenerates (DD)

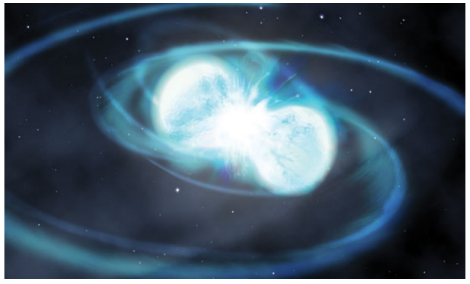

WD Mergers

- Merger – the merger of two sub-Chandrasekhar mass CO WDs in a close binary, triggers a carbon detonation in the more massive of the WDs.
- SubChDet – sub-Chandrasekhar mass model with centrally ignited detonations
- SubChDoubleDet – double detonation model, where the carbon detonation in the core of the sub-Chandrasekhar mass WD is triggered by an initial detonation in a He surface layer that has been accreted from a binary companion.

SN Ia: Carbon deflagration: W7

Despite its parametrized description of the thermonuclear burning process in 1D, the ejecta structure of the so-called W7 model of Nomoto et al. (1984) has been quite successful in reproducing observations of normal SNe Ia. W7 is considered as a standard theoretical reference model for the thermonuclear explosion of M_{Ch} CO WDs.

In this work, we use the revised version of this model published by Iwamoto et al. (1999), which includes an extended nucleosynthesis calculation.

The model contains 0.59 $M_\odot$ of ^{56}Ni located in a shell roughly between 2700 and 11 000 km s^{-1}. While the innermost regions are composed of stable iron, a region rich in intermediate mass elements (IME) lies on top of the nickel shell. Finally, the outermost zones of the W7 model have not burnt and are thus composed entirely of CO fuel.

SN Ia: Delayed detonation: N100

Delayed detonations have long been considered as the most promising mechanism to explain normal SNe Ia for M_{Ch} CO WD progenitors.

In this scenario, the thermonuclear flame first propagates as a subsonic deflagration which later transitions into a detonation.

For this work we use the N100 model, computed by Röpke et al. (2012) and reproduced the observations of SN 2011fe. The initial deflagration is triggered in 100 ignition spots distributed randomly in the centre of a M_{Ch} CO WD.

After the deflagration and successive detonation stage a total of 0.60 $M_\odot$ of radioactive nickel have been synthesized in the explosion.

SN Ia: Violent merger

The violent merger scenario
constitutes an alternative route to SNe Ia.

In this scenario,
the merger of two CO WDs in
a close binary, triggers a carbon detonation
in the more massive of the WDs,
which, in turn, disrupts the whole system.

Pakmor et al. (2012) presented
a binary configuration consisting of a
0.9 and a 1.1 $M_\odot$ CO WD, which produced
0.61 $M_\odot$ of ^{56}Ni and explains the optical
spectra of normal SNe Ia reasonably well.

For this work, we adopt this model
as an example of the merger scenario.

Pakmor et al.(2012)

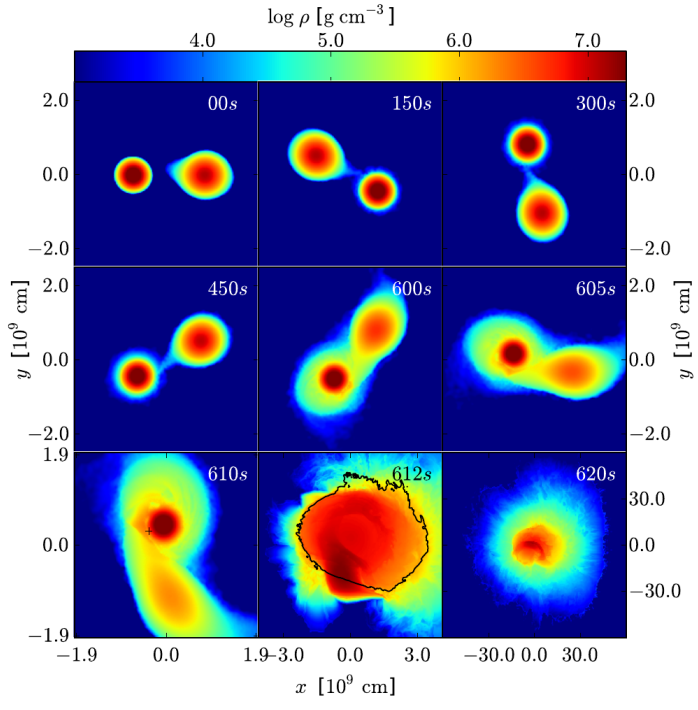

SN Ia: Sub-Chandrasekhar mass detonation model

Shigeyama et al. (1992) and Sim et al. (2010) showed that centrally ignited detonations in sub-Chandrasekhar mass CO WDs successfully reproduce important characteristics of normal SNe Ia. It's highlighting the potential significance of sub-Chandrasekhar models as progenitors for SNe Ia.

Here, we pick two models to investigate the early-time observables of both bare CO detonations and double detonations in sub-Chandrasekhar mass WDs.

As a bare CO detonation, we use the model (SubChDet) of a detonation of a $1.06 M_\odot$ WD that yields $0.56 M_\odot$ of ^{56}Ni (model 1.06 of Sim et al. 2010).

SN Ia: the double detonation model

In the double
detonation scenario a surface detonation
in a helium layer initiates a detonation
in the underlying carbon/oxygen
core leading to an explosion.

We take the model 3 of Fink et al. (2010), which yields $0.55 M_\odot$ of ^{56}Ni from an initial WD with a $1.03 M_\odot$ CO core and a He shell of $5.5 \times 10^{-2} M_\odot$ (SubChDoubleDet).

In the initial helium-shell detonation, $1.7 \times 10^{-3} M_\odot$ of ^{56}Ni, $5.6 \times 10^{-3} M_\odot$ of ^{52}Fe and $4.0 \times 10^{-3} M_\odot$ of ^{48}Cr have been synthesized close to the ejecta surface.

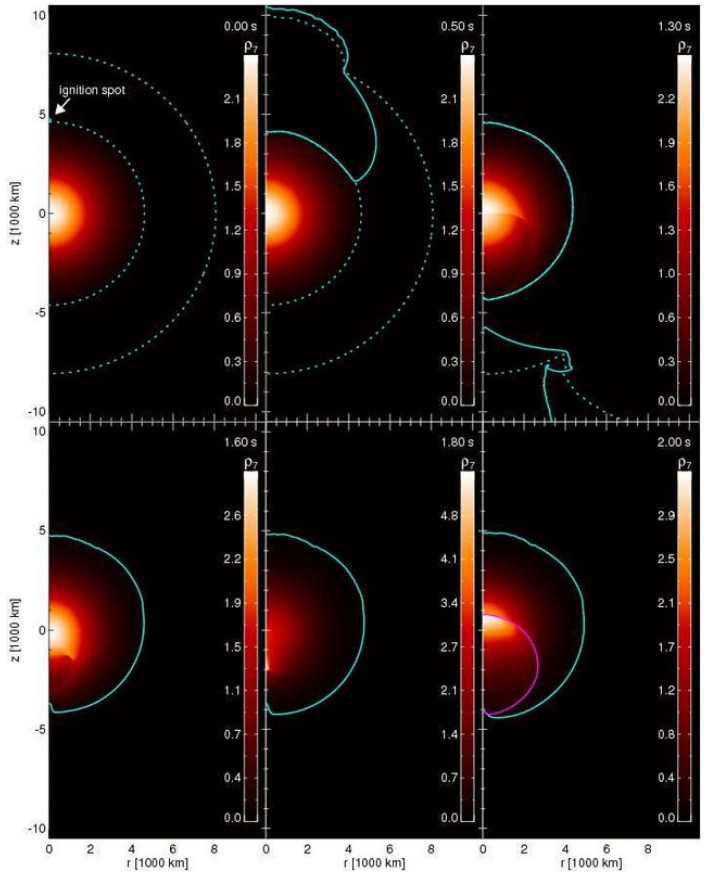

Fink et al.(2010)

Key properties of the models

Model	M_{tot}	M_{56Ni}	E_{kin}	Ref
W7	1.380	0.587	1.103	Iwamoto et al. (1999)
N100	1.406	0.604	1.424	Seitenzahl et al. (2013)
Merger	1.935	0.613	1.607	Pakmor et al. (2012)
SubChDet	1.062	0.559	0.978	Sim et al. (2010)
SubChDoubleDet	1.095	0.549	1.230	Fink et al. (2010)

M — in units of $M_\odot$,
E_{kin} — in units of $\times 10^{51} ergs$,
t_{stop} — the time until which the original explosion simulation was performed.

Key properties of the models: density profiles

Overview the model density profiles.

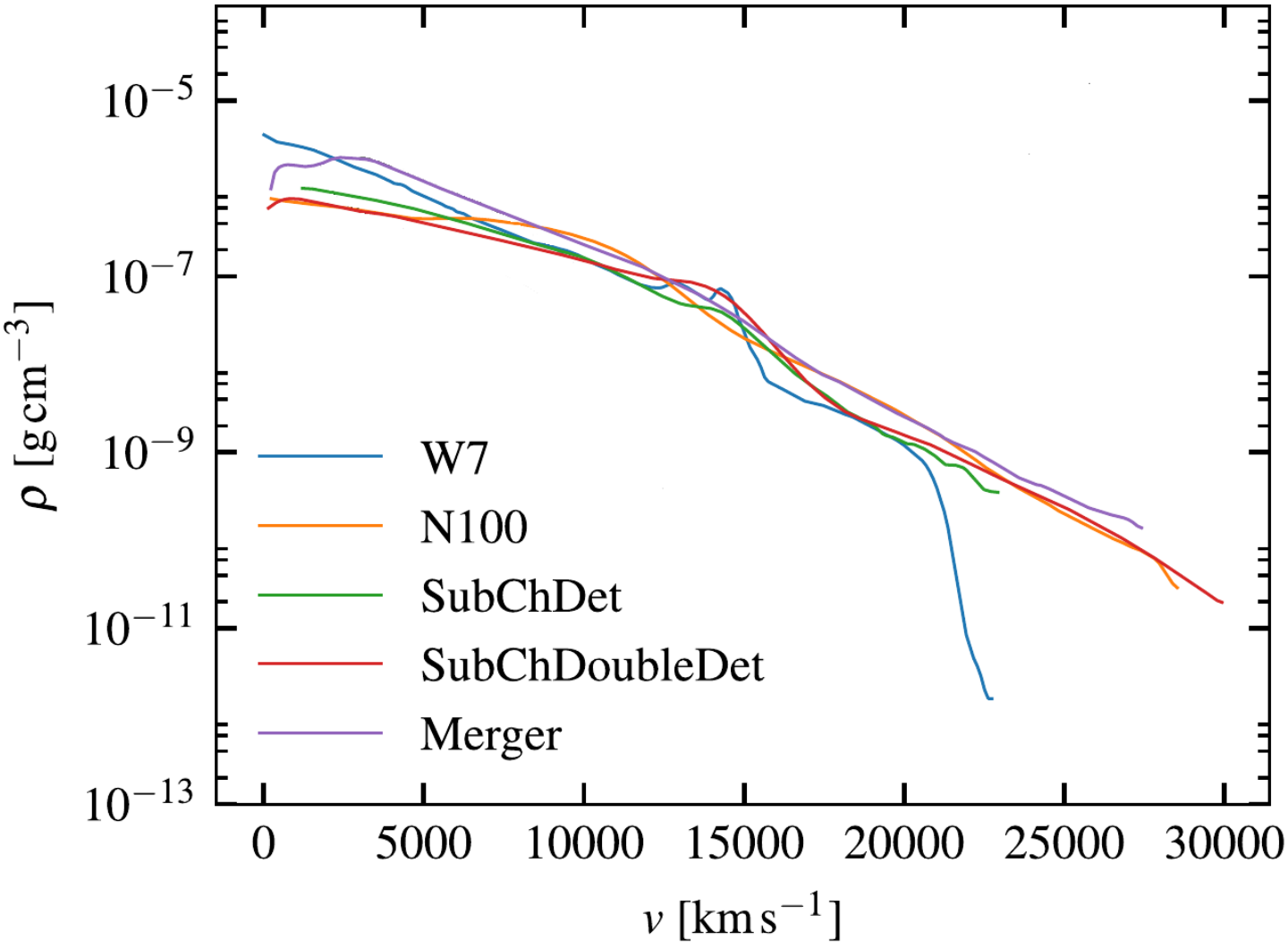

Code STELLA: in details

The light curves of the models was computed by a multi-group radiation hydrodynamics code STELLA after mapping initial models on to an one-dimensional spherical grid.

The code STELLA is developed by ITEP group led by prof. S.Blinnikov.

STELLA employs a direct numerical solution of radiative transfer equations in the moment approximation. STELLA is not a Monte Carlo code.

The system of time-dependent transfer equations:

$$
\begin{cases}
\frac{\partial r}{\partial t} & = u \\
\frac{\partial u}{\partial t} & = -4\pi r^2 \frac{\partial (p+q)}{\partial m} - \frac{Gm}{r^2} + a_{\rm r} + a_{\rm mix} \\
\frac{\partial T}{\partial t} & = \left(\frac{\partial e}{\partial T}\right)_{\rho}^{-1} \left(\varepsilon + 4\pi \int_0^{\infty} \chi_{\rm a} \frac{J_\nu - B_\nu}{\rho} d\nu - 4\pi \frac{\partial r^2 u}{\partial m} \left[T \left(\frac{\partial p}{\partial T} \right)_{\rho} + q \right] \right) \\
\frac{\partial \mathcal{J}_\nu}{\partial t} & = -\frac{c}{r^2} \cdot \frac{\partial}{\partial r}(r^2 \mathcal{H}_\nu) + c(\bar{\eta}_\nu - \chi_{\rm a} \mathcal{J}_\nu) + \frac{u}{r}(3\mathcal{K}_\nu - \mathcal{J}_\nu) - \\
 & \quad -\frac{1}{r^2} \cdot \frac{\partial}{\partial r}(r^2 u)(\mathcal{J}_\nu + \mathcal{K}_\nu) - \\
 & \quad -\frac{1}{\nu^3} \cdot \frac{\partial}{\partial \nu} \nu^4 \left[\frac{u}{r}(3\mathcal{K}_\nu - \mathcal{J}_\nu) - \frac{1}{r^2} \cdot \frac{\partial}{\partial r}(r^2 u) \mathcal{K}_\nu \right] \\
\frac{\partial \mathcal{H}_\nu}{\partial t} & = -c \frac{\partial \mathcal{K}_\nu}{\partial r} - \frac{c}{r}(3\mathcal{K}_\nu - \mathcal{J}_\nu) - 2\left(\frac{u}{r} + \frac{\partial u}{\partial r} \right) \mathcal{H}_\nu - \\
 & \quad -c(\chi_{\rm a} + \chi_{\rm s}) \mathcal{H}_\nu + \dot{\mathcal{H}}_{\nu_{\rm diff}}
\end{cases}
$$

Modelling assumptions & limitations

STELLA solves the time-dependent equations implicitly for the angular moments of intensity averaged over fixed frequency groups.
Hydrodynamics coupled to radiation is fully computed (homologous expansion is not assumed).

Modelling assumptions

- The equations were written in one-dimensional spherical geometry.
- The levels and ions populations are computed under LTE.
- Our total opacity included contributions from photoionization, bremsstrahlung, lines (as expansion opacity), and e-scattering.
- The line opacity with expansion effect in lines was computed using atomic data from the Kuruzc's list with approximately 150,000 lines.

No assumption of radiative equilibrium. The photon energy distribution may be quite arbitrary.
We used 200 frequency groups, which are logarithmically distributed between 40 to 50000 Å.

Synthetic light curves in the UBVR passbands

The resulting light curves in the Bessell U, B, V and R bands of all models for the first 10 days after explosion.

The LC shapes are similar, with the exception of the DD model.

For DD model the radioactive material is close to the surface. It leads to first peaks or shoulders in the light curves.

The differences in the rise are clearly seen.

There is a spread of about $\Delta t \sim 0.6d$ for the time when the light curves reach an absolute magnitude of $M_{AB} = -10$ in the V band.

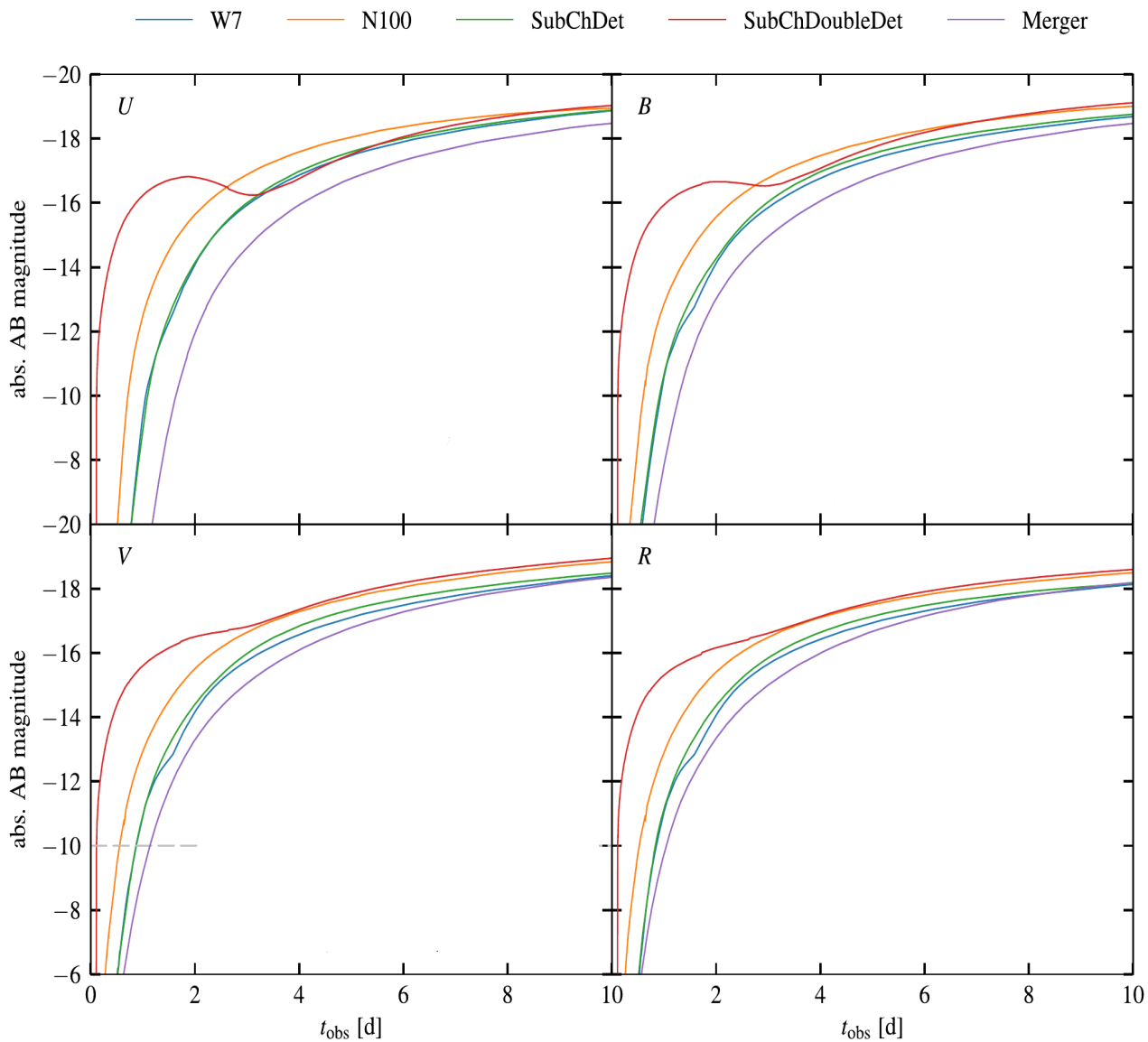

Rising phase

There are differences in the time when a certain absolute magnitude ($V = -10^m$, arbitrarily chosen) is reached.

The largest difference at $V = -10^m$ $\Delta t = 0.6$ d

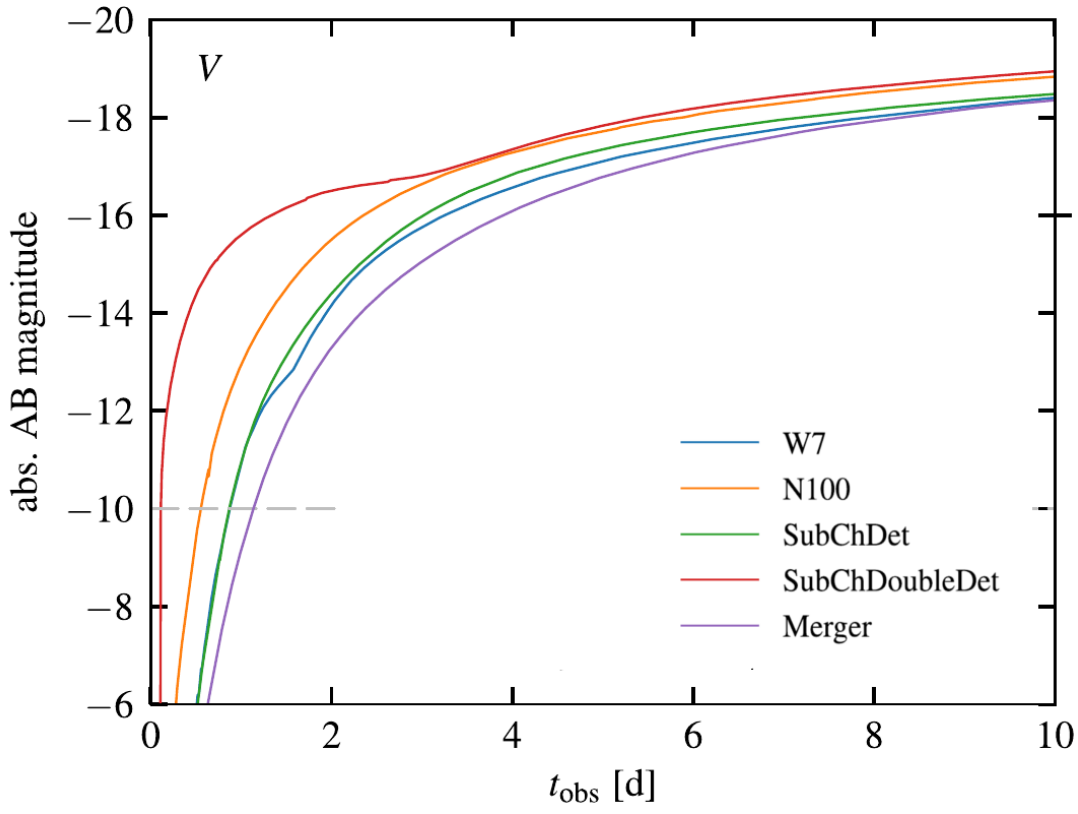

Rising phase

There are differences in the time when a certain absolute magnitude ($V = -10^m$, arbitrarily chosen) is reached.

The largest difference at $V = -10^m$ $\Delta t = 0.6$ d

The reason is the different distributions of ^{56}Ni.

Column density:

$$n = \int_{r_{^{56}Ni}}^{r_{out}} dr \rho(r)$$

where
$r_{^{56}Ni} = r(X_{^{56}Ni} > 0.01)$

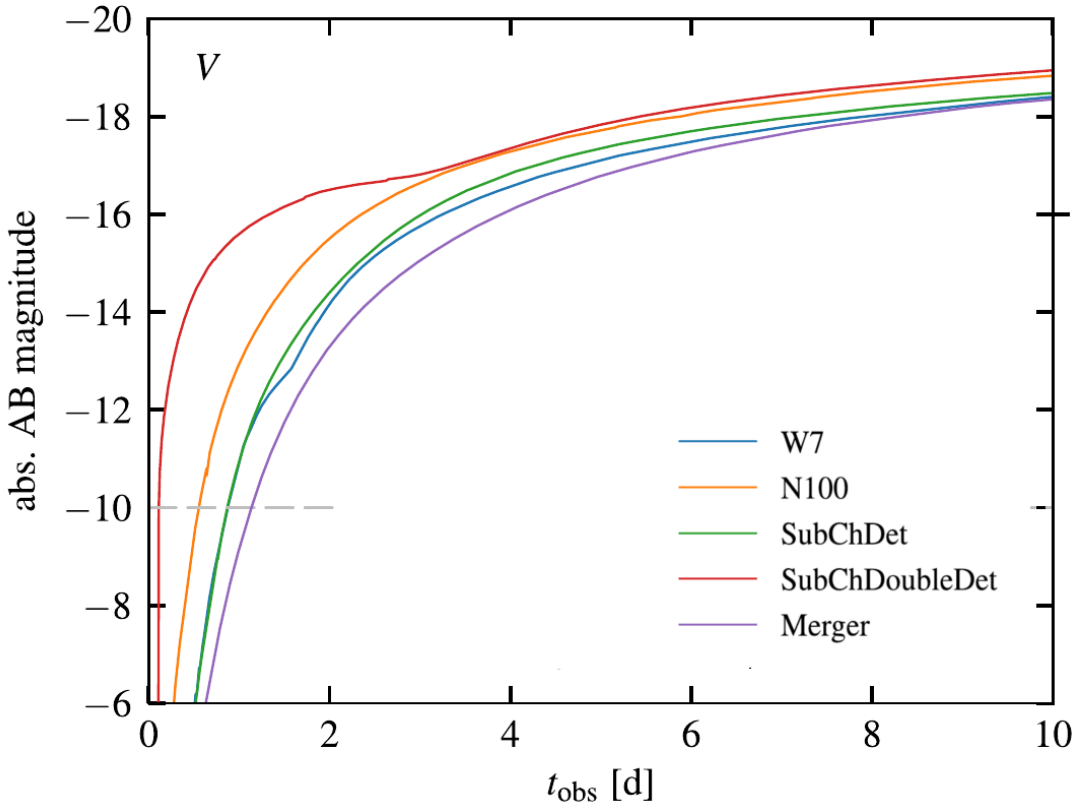

Rising phase

There are differences in the time when a certain absolute magnitude ($V = -10^m$, arbitrarily chosen) is reached.

The largest difference at $V = -10^m$ $\Delta t = 0.6$ d

The reason is the different distributions of ^{56}Ni.

Column density:

$$n = \int_{r_{^{56}Ni}}^{r_{out}} dr\rho(r)$$

where
$r_{^{56}Ni} = r(X_{^{56}Ni} > 0.01)$

Correlation between the time since explosion until an absolute magnitude of $M = -10$ is reached in the V band and the column density n:

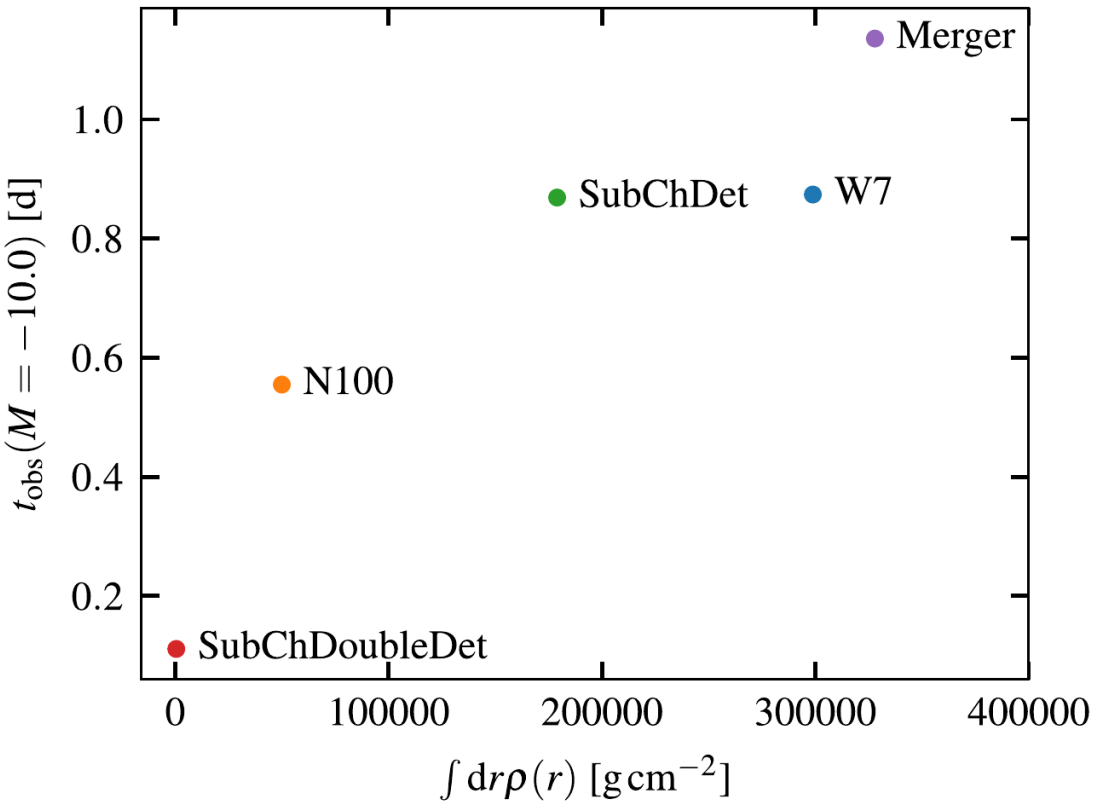

Explosion time fitting

SN 2011fe

Nugent et al. (Nature, 2011)

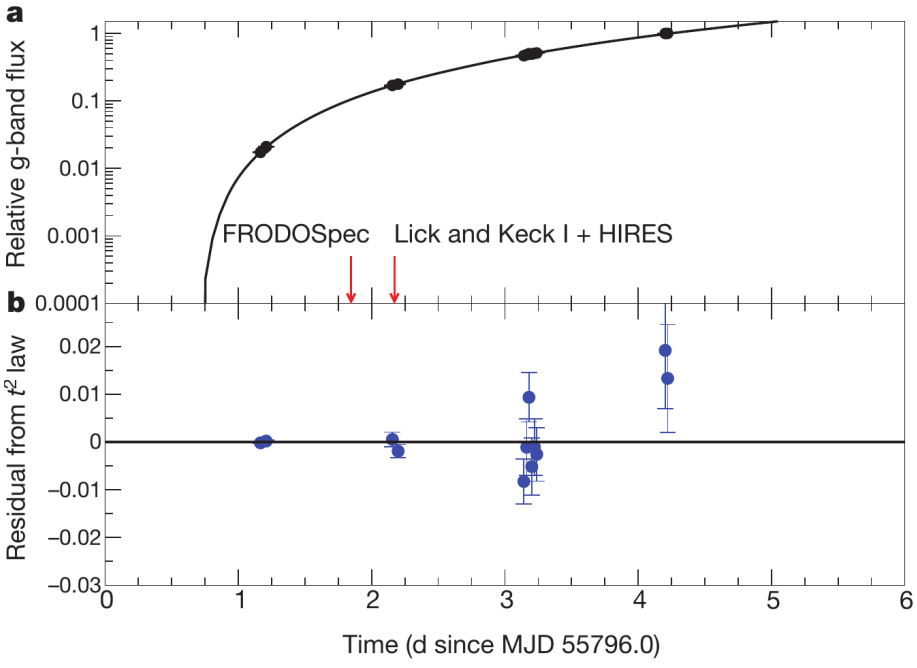

Figure 3 | Early photometry of SN 2011fe shows a parabolic rise and constrains the time of explosion. **a**, Relative g-band flux as a function of time for the first four nights after detection. Here we have fit the rise with a t^2 fireball model: we assume that the flux is proportional to $(t - t_{\mathrm{expl}})^2$, where t_{expl} denotes the time of explosion. **b**, Residuals from the fit.

The early-time light curve allows Nugent et al. to put the constrains on the progenitor radius.
"The day 0.45 g-band observation of SN 2011fe indicates $L \sim 10^{40}$ ergs/s, which constrains the progenitor radius:"

$$R_0 \leq 10^{10} cm$$

It's the direct evidence that the progenitor was a compact star, namely WD.

It's typically to obtain the time explosion from observation by fitting a power law to early-time light curve and extrapolating to $L(t) = 0$.
From Nugent et al.(2011):

Using this 't^2 model', we find an explosion time at modified Julian date (MJD) 55796.696 ± 0.003 (Fig. 3). Letting the exponent of the power law differ from two, which captures some of the deviations from the fireball model, and fitting just the first three nights of data, results in a best-fit explosion date of MJD 55796.687 ± 0.014 (2011 August 23, 16:29 ± 20 min UT).

Explosion time fitting

SN 2011fe

Nugent et.al. (Nature, 2011)

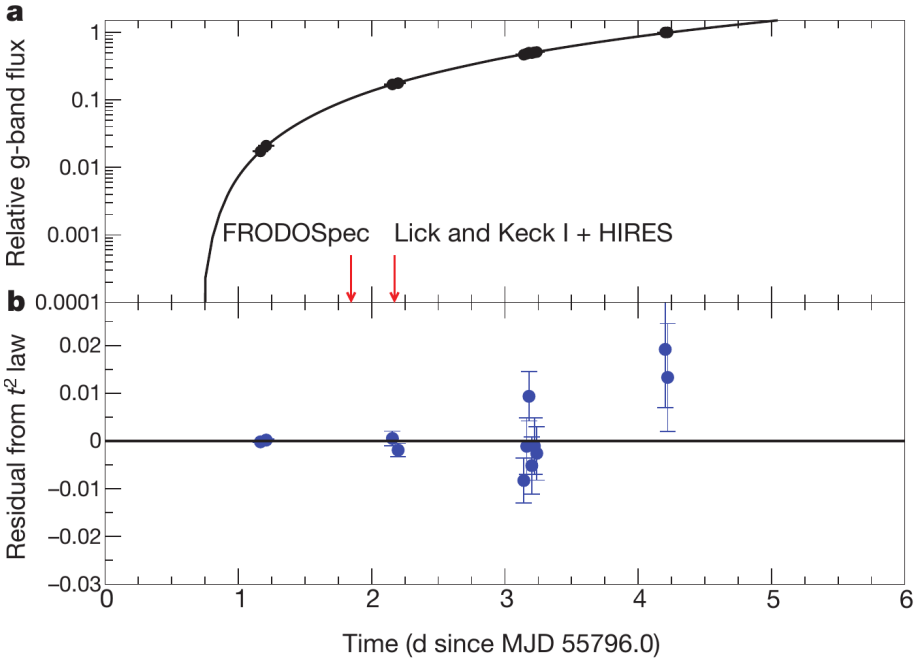

Figure 3 | Early photometry of SN 2011fe shows a parabolic rise and constrains the time of explosion. **a**, Relative g-band flux as a function of time for the first four nights after detection. Here we have fit the rise with a t^2 fireball model: we assume that the flux is proportional to $(t - t_{\mathrm{expl}})^2$, where t_{expl} denotes the time of explosion. **b**, Residuals from the fit.

Fireball model:

$$M_{FL} = a - 2.5 \log_{10}(t + \delta t)^2$$

Power law with an arbitrary constant exponent p:

$$M_{PL} = a - 2.5 \log_{10}(t + \delta t)^p$$

Minimize:

$$\chi^2 = \sum \left(M_i^{obs} - M_i^{fit} \right)^2$$

Explosion time fitting

Very good fit can be achieved with both the fireball and the power-law models. The accuracy is in the insets. The time of explosion cannot be accurately reconstructed in most cases

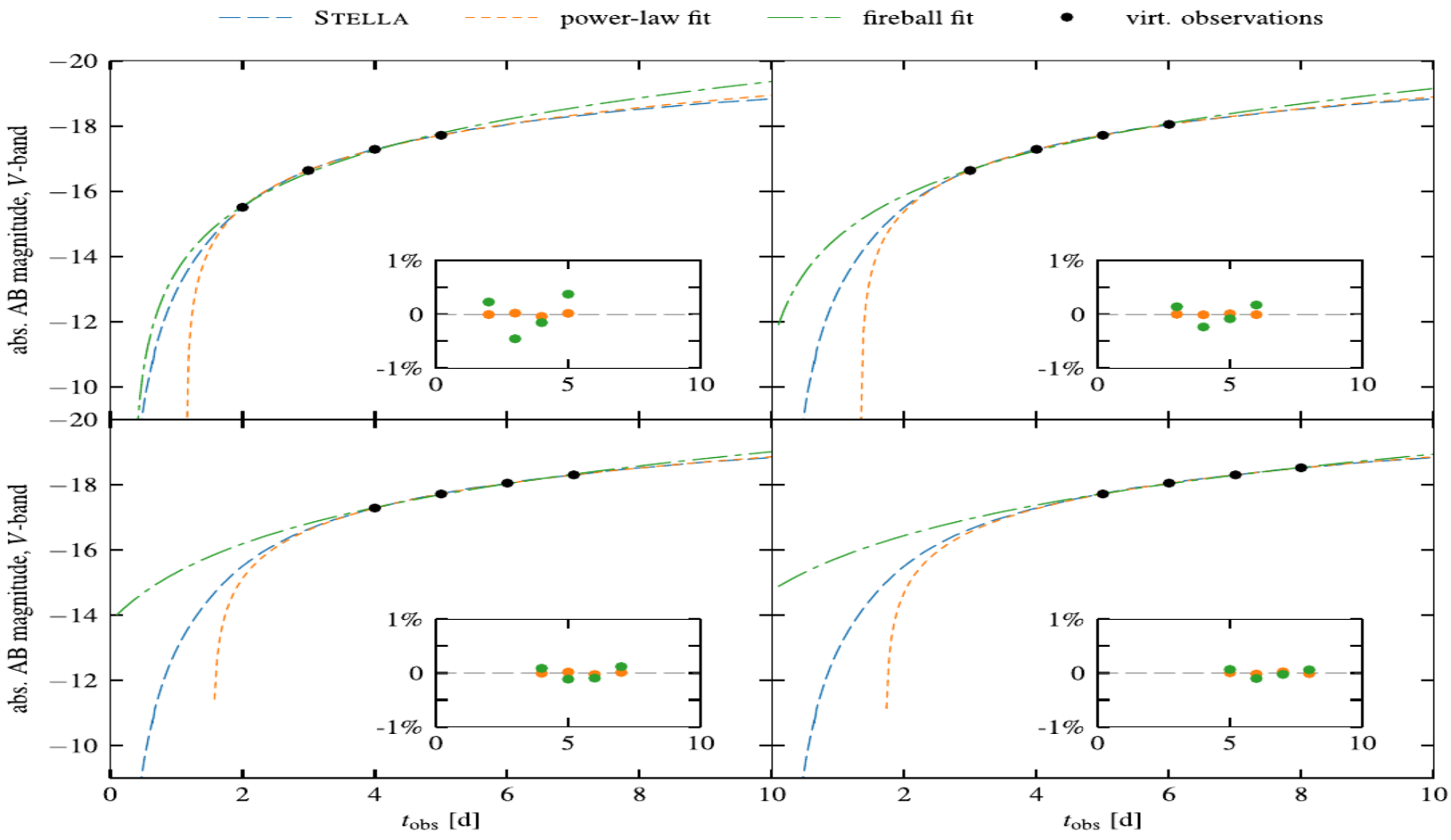

Explosion time fitting

Illustration of the offset between reconstructed and real times of explosion for all models.
The different panels show histograms of obtained for all models for different assumptions about the time of first observation after explosion t(obs). From left to right, top to bottom, t(obs) increases from 2 to 5 d in 1 d increments.

The results for the power-law fit are shown in blue and the corresponding results for the fireball model fit in orange.

The offset between reconstructed and real times of explosion.

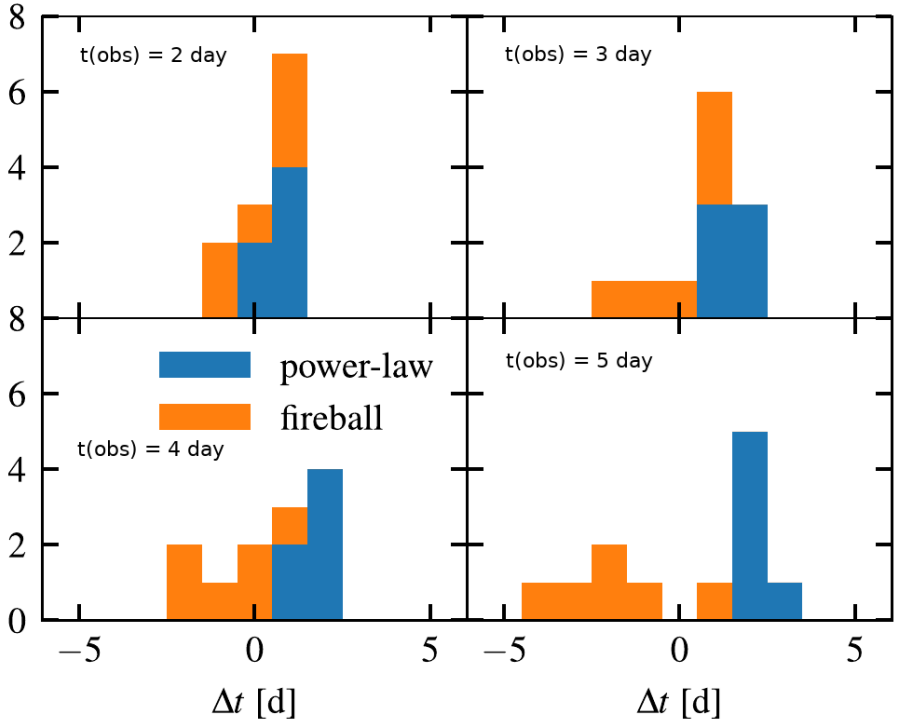

This overview clearly highlights the difficulty in reconstructing the explosion time from fits to the early light curve.

SN Ia: the double detonation model

The carbon detonation in the core of the sub-Chandrasekhar mass WD is triggered by an initial detonation in a He surface layer. He has been accreted from a binary companion.

For the double detonation scenario (SubChDoubleDet), we take model 3 of Fink et al. (2010), which yields $0.55 M_\odot$ of ^{56}Ni from an initial WD with a $1.03 M_\odot$ CO core and a He shell of $5.5 \times 10^{-2} M_\odot$.

In the initial helium-shell detonation have been synthesized close to the ejecta surface:

Isotope	Mass at surface
^{56}Ni	$1.7 \times 10^{-3} M_\odot$
^{52}Fe	$5.6 \times 10^{-3} M_\odot$
^{48}Cr	$4.0 \times 10^{-3} M_\odot$

Abundances of SubChDoubleDet

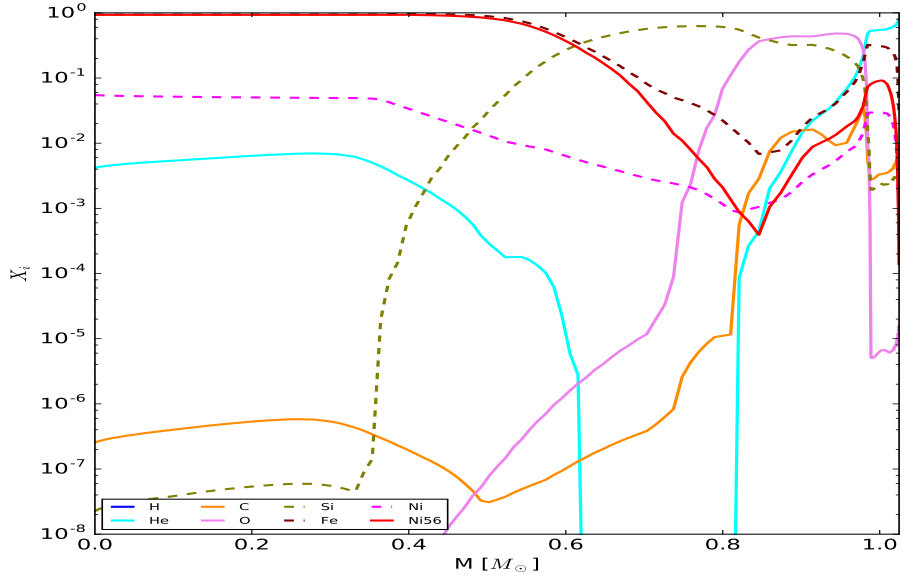

The importance of the two additional decay chains: ^{52}Fe and ^{48}Cr

Decay chain		T1/2	Q	M
^{56}Ni → ^{56}Co → ^{56}Fe	Ni56:	6.075 d	1.718 MeV	55.94 u
	Co56:	77.23 d	3.633 MeV	55.94 u
^{52}Fe → ^{52}Mn → ^{52}Cr	Fe52:	8.275 h	0.751 MeV	51.95 u
	Mn52:	21.1 min	2.447 MeV	51.95 u
^{48}Cr → ^{48}V → ^{48}Ti	Cr48:	21.56 h	0.432 MeV	47.95 u
	V48:	15.9735 d	2.910 MeV	47.95 u

The rates of energy production

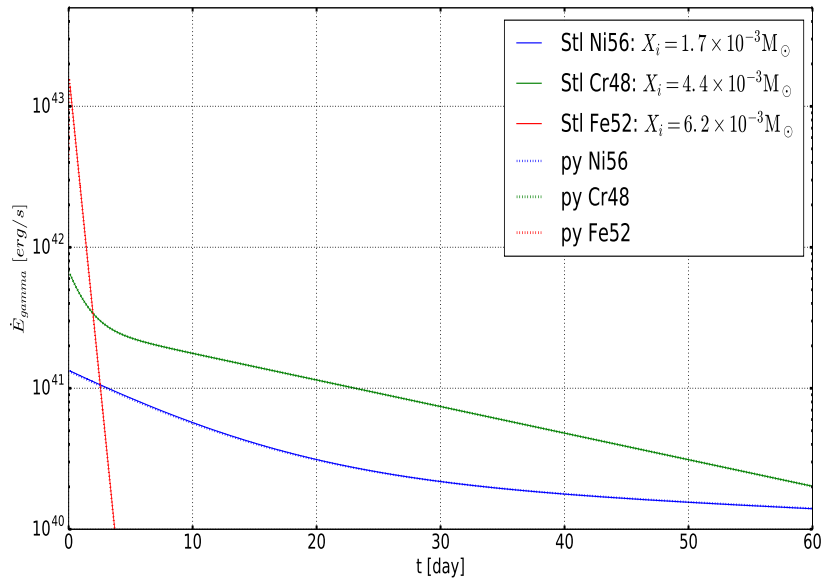

U band early light curve

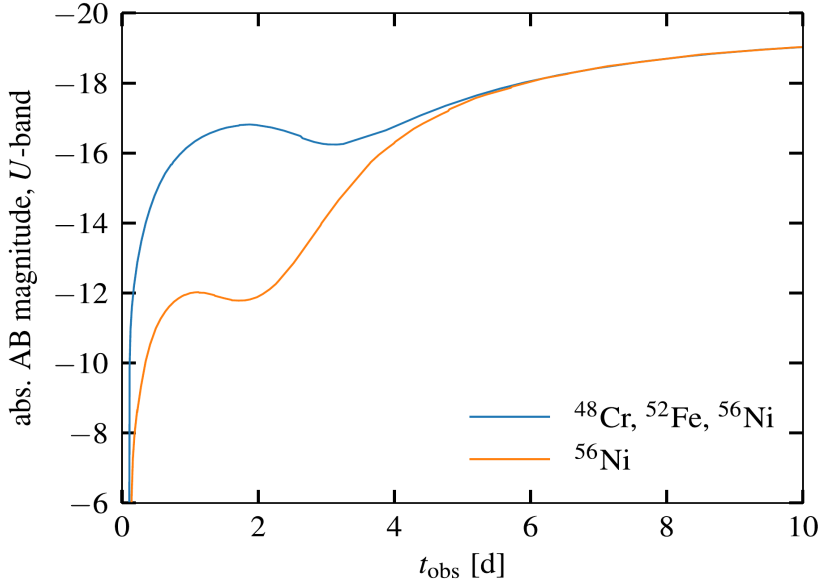

Double detonation: synthetic light curves

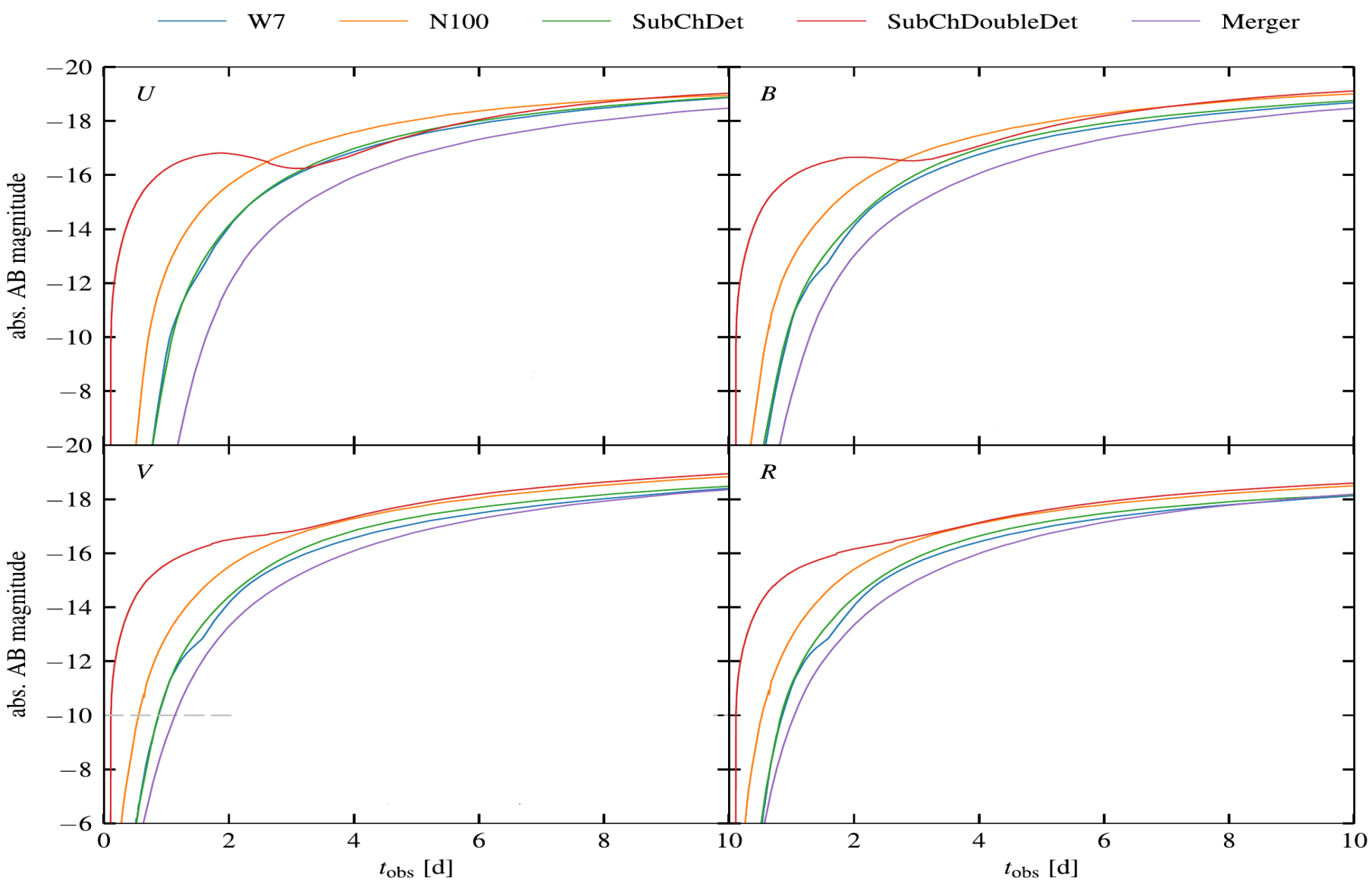

The SED and U—V colour evolution

U—V colour evolution in the double detonation (SubChDoubleDet), the N100 and the W7 models.

The SED at the moments: 2^d, 5^d

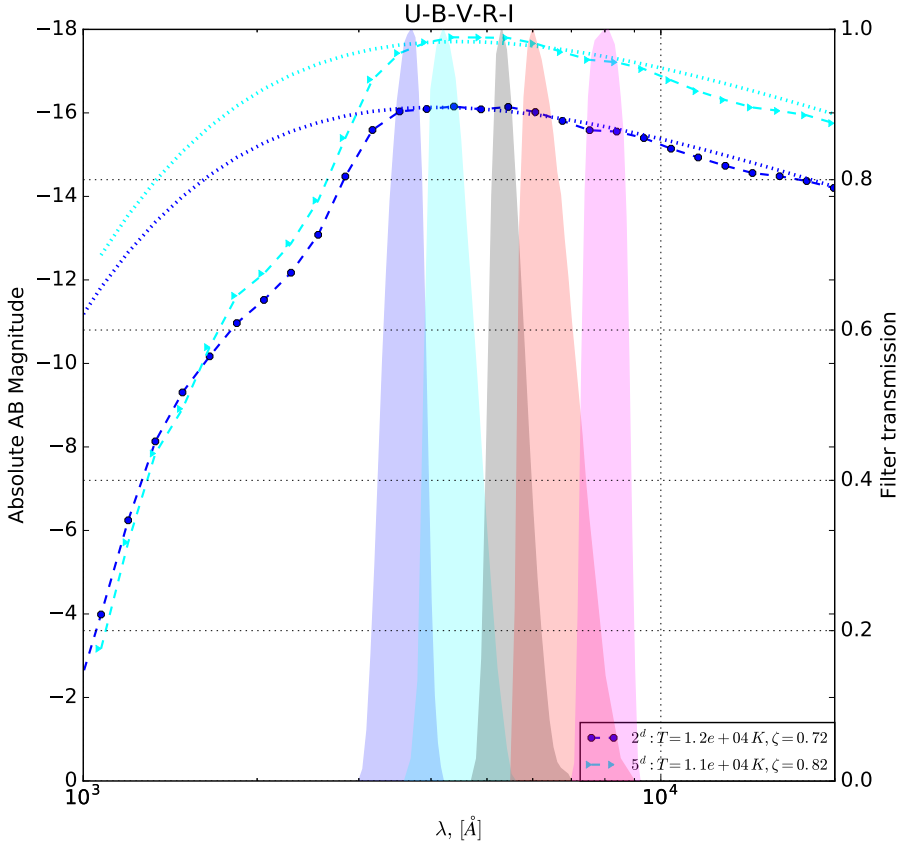

The prompt emission due to the radioactive material at the ejecta surface leads to a blue colour in the double-detonation model very early on.

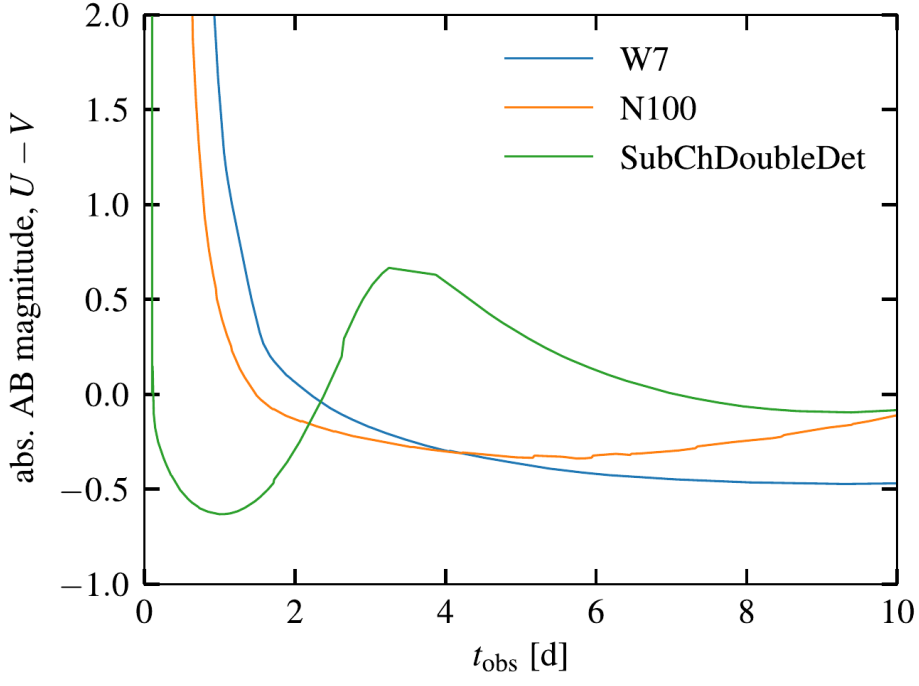

Double Detonation: remarks

Imprint of double-detonation mechanism in early light curves for Type Ia supernovae: radioactive material close to the surface leads to a fast and very early rise of the light curve or even a first maximum.

Similar behavior is predicted for the interaction between ejecta and a companion (Kasen, AJ, 2010)
OR
between ejecta and CSM (Piro & Morozova, A&A, 2016).

BUT
Detection narrow emission lines in early spectra would be strong argument for ejecta-CSM interaction.

BUT
The early observation of γ-lines may confirm the closeness of radioactive material to the surface.
It's possible for the nearest supernovae, e.g. SN 2014J.

Surface Radioactivity or Interactions?

Surface Radioactivity or Interactions? Multiple Origins of Early-excess Type Ia Supernovae and Associated Subclasses.

J. Jiang, M. Doi, K. Maeda, T. Shigeyama

The Astrophysical Journal, 865(2), 149.
http://doi.org/10.3847/1538-4357/aadb9a

Early-phase Type Ia supernovae (SNe Ia), especially those with luminosity enhancement within the first few days of explosions ("early-excess SNe Ia"), play an irreplaceable role in addressing the long-standing progenitor and explosion issue of SNe Ia. In this paper, we systematically investigate 11 early-excess SNe Ia from subluminous to luminous subclasses. Eight of them are selected from 23 SNe Ia with extremely early-phase optical light curves ("golden" early-phase SNe Ia), and three of them are selected from 40 SNe Ia (including 14 golden samples) with early-phase UV/NUV light curves. We found that previously discovered early-excess SNe Ia show a clear preference for specific SN Ia subclasses. In particular, the early-excess feature shown in all six luminous (91T- and 99aa-like) SNe Ia is in conflict with the viewing angle dependence predicted by the companion-ejecta interaction scenario. Instead, such a high early-excess fraction is likely related to the explosion physics of luminous SNe Ia; i.e., a more efficient detonation happening in the progenitor of luminous SNe Ia may consequently account for the early-excess feature powered by the radiation from a ^{56}Ni-abundant outer layer. The diversity of early-excess features shown in different SN Ia subclasses suggests multiple origins of the discovered early-excess SNe Ia, challenging their applicability as a robust progenitor indicator. Further understanding of the early-excess diversity relies not only on multiband photometry and prompt-response spectroscopy of individual early-excess SNe Ia but also on investigations of the general early-phase light-curve behavior of each SN Ia subclass, which can be realized through ongoing/forthcoming transient survey projects in the near future.

Surface Radioactivity or Interactions?

Surface Radioactivity or Interactions? Multiple Origins of Early-excess Type Ia Supernovae and Associated Subclasses.
J. Jiang, M. Doi, K. Maeda, T. Shigeyama
The Astrophysical Journal, 865(2), 149.
http://doi.org/10.3847/1538-4357/aadb9a

Early-phase Type Ia supernovae (SNe Ia), especially those with luminosity enhancement within the first few days of explosions ("early-excess SNe Ia"), play an irreplaceable role in addressing the long-standing progenitor and explosion issue of SNe Ia. In this paper, we systematically investigate 11 early-excess SNe Ia from subluminous to luminous subclasses. Eight of them are selected from 23 SNe Ia with extremely early-phase optical light curves ("golden" early-phase SNe Ia), and three of them are selected from 40 SNe Ia (including 14 golden samples) with early-phase UV/NUV light curves. We found that previously discovered early-excess SNe Ia show a clear preference for specific SN Ia subclasses. In particular, the early-excess feature shown in all six luminous (91T- and 99aa-like) SNe Ia is in conflict with the viewing angle dependence predicted by the companion-ejecta interaction

Instead, such a high early-excess fraction is likely related to the explosion physics of luminous SNe Ia; i.e., a more efficient detonation happening in the progenitor of luminous SNe Ia may consequently account for the early-excess feature powered by the radiation from a ^{56}Ni-abundant outer layer.

challenging their applicability as a robust progenitor indicator. Further understanding of the early-excess diversity relies not only on multiband photometry and prompt-response spectroscopy of individual early-excess SNe Ia but also on investigations of the general early-phase light-curve behavior of each SN Ia subclass, which can be realized through ongoing/forthcoming transient survey projects in the near future.

SN 2018oh

K2 Observations of SN 2018oh Reveal a Two-component Rising Light Curve for a Type Ia Supernova.
The Astrophysical Journal, 870(1), L1.
http://doi.org/10.3847/2041-8213/aaedb0

We present an exquisite 30 minute cadence *Kepler* (K2) light curve of the Type Ia supernova (SN Ia) 2018oh (ASASSN-18bt), starting weeks before explosion, covering the moment of explosion and the subsequent rise, and continuing past peak brightness. These data are supplemented by multi-color Panoramic Survey Telescope (Pan-STARRS1) and Rapid Response System 1 and Cerro Tololo Inter-American Observatory 4 m Dark Energy Camera (CTIO 4-m DECam) observations obtained within hours of explosion. The K2 light curve has an unusual two-component shape, where the flux rises with a steep linear gradient for the first few days, followed by a quadratic rise as seen for typical supernovae (SNe) Ia. This "flux excess" relative to canonical SN Ia behavior is confirmed in our *i*-band light curve, and furthermore, SN 2018oh is especially blue during the early epochs. The flux excess peaks 2.14 ± 0.04 days after explosion, has a FWHM of 3.12 ± 0.04 days, a blackbody temperature of $T = 17,500^{+11,500}_{-9,000}$ K, a peak luminosity of $4.3 \pm 0.2 \times 10^{37}$ erg s^{-1}, and a total integrated energy of $1.27 \pm 0.01 \times 10^{43}$ erg. We compare SN 2018oh to several models that may provide additional heating at early times, including collision with a companion and a shallow concentration of radioactive nickel. While all of these models generally reproduce the early K2 light curve shape, we slightly favor a companion interaction, at a distance of $\sim 2 \times 10^{12}$ cm based on our early color measurements, although the exact distance depends on the uncertain viewing angle. Additional confirmation of a companion interaction in future modeling and observations of SN 2018oh would provide strong support for a single-degenerate progenitor system.

SN 2018oh

K2 Observations of SN 2018oh Reveal a Two-component Rising Light Curve for a Type Ia Supernova.
The Astrophysical Journal, 870(1), L1.
http://doi.org/10.3847/2041-8213/aaedb0

We present an exquisite 30 minute cadence *Kepler* (K2) light curve of the Type Ia supernova (SN Ia) 2018oh (ASASSN-18bt), starting weeks before explosion, covering the moment of explosion and the subsequent rise, and continuing past peak brightness. These data are supplemented by multi-color Panoramic Survey Telescope (Pan-STARRS1) and Rapid Response System 1 and Cerro Tololo Inter-American Observatory 4 m Dark Energy Camera (CTIO 4-m DECam) observations obtained within hours of explosion. The K2 light curve has an unusual two-component shape, where the flux rises with a steep linear gradient for the first few days, followed by a quadratic rise as seen for typical supernovae (SNe) Ia. This "flux excess" relative to canonical SN Ia behavior is confirmed in

our *i*-band light curve, and furthermore, SN 2018oh is especially blue during the early epochs. The
peaks 2.14 ± 0.04 days after explosion, has a FWHM of 3.12 ± 0.04 days, a blackbody ter
$T = 17,500^{+11,500}_{-9,000}$ K, a peak luminosity of $4.3 \pm 0.2 \times 10^{37}$ erg s^{-1}, and a total integrated
$1.27 \pm 0.01 \times 10^{43}$ erg. We compare SN 2018oh to several models that may provide additional hea

of $\sim 2 \times 10^{12}$ cm based on our early color measurements, although the exact distance depends on the uncertain viewing angle. Additional confirmation of a companion interaction in future modeling and observations of SN 2018oh would provide strong support for a single-degenerate progenitor system.

SN 2018oh

K2 Observations of SN 2018oh Reveal a Two-component Rising Light Curve for a Type Ia Supernova.
The Astrophysical Journal, 870(1), L1.
http://doi.org/10.3847/2041-8213/aaedb0

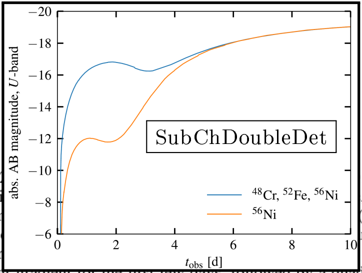

We present an exquisite 30 minute cadence *Kepler* (K2 … 18oh (ASASSN-18bt), starting weeks before explosion, coveri… , and continuing past peak brightness. These data are supplem… (Pan-STARRS1) and Rapid Response System 1 and Cerro Tol… mera (CTIO 4-m DECam) observations obtained within hour… two-component shape, where the flux rises with a steep linear gradient for the first few days, followed by a quadratic rise as seen for typical supernovae (SNe) Ia. This “flux excess” relative to canonical SN Ia behavior is confirmed in

our *i*-band light curve, and furthermore, SN 2018oh is especially blue during the early epochs. The peaks 2.14 ± 0.04 days after explosion, has a FWHM of 3.12 ± 0.04 days, a blackbody ter $T = 17,500^{+11,500}_{-9,000}$ K, a peak luminosity of $4.3 \pm 0.2 \times 10^{37}$ erg s^{-1}, and a total integrated $1.27 \pm 0.01 \times 10^{43}$ erg. We compare SN 2018oh to several models that may provide additional hea

of $\sim 2 \times 10^{12}$ cm based on our early color measurements, although the exact distance depends on the uncertain viewing angle. Additional confirmation of a companion interaction in future modeling and observations of SN 2018oh would provide strong support for a single-degenerate progenitor system.

Conclusions

- ✓ We provide predictions for early light curves for a number of SN Ia explosion models based on detailed radiative transfer simulations.
- ✓ Similar light curve evolution during the early phase for most of the examined models. There are differences in the time when a certain absolute magnitude ($V = -10^m$) is reached.
- ✓ None of the synthetic light curves exhibit the commonly assumed power-law rise. Using power-law rise the time of SN Ia explosion could be determined with substantial errors.
- ✓ Imprint of double-detonation mechanism in early light curves for Type Ia supernovae: radioactive material close to the surface leads to a fast and very early rise of the light curve or even a first maximum.
- ✓ Alone the photometry is not enough to identify certain explosion scenarios. We need spectra and appearance in the $\gamma-$ or X-ray regimes.
- ✓ All our models are available online at: https://hesma.h-its.org
- ✓ arxiv:1706.03613
- ✓ Thank you for your attention!